Characterization of S818L mutation in *HERG* C-terminus in LQT2

Modification of activation–deactivation gating properties

Tadashi Nakajima[a], Masahiko Kurabayashi[a,*], Yoshio Ohyama[a], Yoshiaki Kaneko[a], Tetsushi Furukawa[b], Toshio Itoh[a], Yasuhiro Taniguchi[a], Toshihiro Tanaka[c], Yusuke Nakamura[c], Masayasu Hiraoka[d], Ryozo Nagai[e]

[a] *Second Department of Internal Medicine, Gunma University School of Medicine, 3-39-15, Showa-Machi, Maebashi, Gunma 371-8511, Japan*
[b] *Department of Physiology, Akita University School of Medicine, Akita, Japan*
[c] *Laboratory of Molecular Medicine, Human Genome Center, Institute of Medical Science, University of Tokyo, Tokyo, Japan*
[d] *Department of Cardiovascular Disease, Medical Research Institute, Tokyo Medical and Dental University, Tokyo, Japan*
[e] *Department of Cardiovascular Medicine, Graduate School of Medicine, University of Tokyo, Tokyo, Japan*

Received 25 July 2000; accepted 14 August 2000

Edited by Maurice Montal

Abstract We examined the mechanism(s) for HERG channel dysfunction in an S818L mutation in the *HERG* C-terminus using the heterologous expression system in *Xenopus* oocytes. Injection of S818L cRNA alone did not produce expressed currents. Coinjection of an equal amount of S818L cRNA with wild-type (WT) cRNA into oocytes did not exhibit apparent dominant-negative suppression. However, coinjection of excess amounts of S818L cRNAs with WT cRNA into oocytes decreased HERG current amplitudes and shifted the voltage dependence of activation to negative potentials, accelerated its activation and deactivation. The data suggest that S818L alone cannot form functional channels, whereas S818L subunits can, at least in part, coassemble with WT subunits to form hetero-tetrameric functional channels, and imply that the *HERG* C-terminus may contain a domain involving the activation–deactivation process of the channel. These findings may provide new insights into the structure–function relationships of the *HERG* C-terminus.

Key words: Long QT syndrome; Potassium channel; C-terminus

1. Introduction

Familial long QT syndrome (LQTS) is an inherited disease characterized by prolongation of ventricular repolarization, frequently associated with lethal ventricular arrhythmias resulting in catastrophic sudden death. Genetic analyses have revealed that the autosomal-dominant trait form of LQTS, Romano–Ward syndrome, is genetically heterogeneous and is linked to at least five different loci (LQT1–LQT5) [1–5]. The human *ether-a-go-go related* gene, *HERG*, is the gene responsible for one form of long QT syndrome (LQT2) and encodes the pore-forming subunit of the rapidly activating delayed rectifier potassium channel (I_{Kr}) in cardiac cells, which is the major determinant of action potential duration [2,6–8].

Many mutations at different sites in *HERG* have been identified in LQT2 patients [2,9–13]. We and other groups have revealed that HERG channel dysfunction in LQT2-associated mutations can be caused by multiple mechanisms [14–22]. Some mutations cause defects in intracellular protein transport to the plasma membrane [17,18]. Others can exist in the plasma membrane thereby producing functional channels with altered gating properties [14,16,20], gain of function due to the altered ion selectivity [20], or non-functional channels in the plasma membrane [17].

From the point of view of primary *HERG* structure, the mechanisms for HERG channel dysfunction could, at least in part, be characterized by the sites at which missense mutations occurred. For example, mutations in the N-terminus accelerated HERG channel deactivation [19], a mutation in the S4 voltage sensor affected the voltage dependence of activation [16], or mutations in the pore region affected HERG channel inactivation [15] or ion selectivity [20]. In contrast, little information is available for characterizing the mechanism(s) for HERG channel dysfunction caused by mutations in the C-terminus. Only mutation V822M has been biochemically and electrophysiologically studied, in which intracellular protein transport to the plasma membrane proved to be defective [17]. Thus, although it is suggested that the *HERG* C-terminus might play a significant role in cardiac repolarization [23], mechanisms for HERG channel dysfunction in mutations in the *HERG* C-terminus are not yet fully understood.

Berthet et al. [23] have recently reported mutation S818L (substitution of serine to leucine at position 818), which is located at the putative cyclic nucleotide binding domain in the *HERG* C-terminus, in LQT2 patients. We have identified this same mutation in Japanese LQT2 patients (unpublished data). Thus, we examined the mechanism(s) for HERG channel dysfunction in the S818L mutation using the heterologous expression system in *Xenopus* oocytes. The data suggest that S818L HERG alone cannot form functional channels. However, S818L subunits can, at least in part, coassemble with wild-type (WT) subunits and produce heteromultimeric functional channels with altered gating properties. These findings may provide new insights into the structure–function relationships of the *HERG* C-terminus.

*Corresponding author. Fax: (81)-27-220 8150.
E-mail: mkuraba@med.gunma-u.ac.jp

PII: S0014-5793(00)01988-8

2. Materials and methods

2.1. Generation of the S818L expression construct

The HERG cDNA clone subcloned into the *Bam*HI–*Eco*RI site of a pGH19 vector was a gift from Dr. Gail A. Robertson (University of Wisconsin). Amino acid substitution of serine to leucine at position 818 within the *HERG* C-terminus was performed by an overlap extension PCR strategy [16]. The insert region, including the cloning sites, of the S818L HERG construct has been sequenced directly.

2.2. Oocyte handling and electrophysiology

Xenopus oocyte preparation and handling were carried out as described previously [15,16]. Briefly, oocytes were surgically removed from *Xenopus laevis* (Hamamatsu Seibutsu) under anesthesia in ice water, washed in Ca^{2+}-free OR2 solution containing (mmol/l) 100 NaCl, 2 KCl, 1 $MgCl_2$, 5 HEPES and 5 Tris (pH 7.6 with HCl). Stage V and VI oocytes were defolliculated by treatment with 2 mg/ml collagenase (type IA, Worthington) in Ca^{2+}-free OR2 solution for 30–60 min, and washed extensively with Ca^{2+}-free OR2 solution containing no collagenase. They were injected with either 40 nl of cRNA encoding WT HERG (0.0375 ng/nl) alone or S818L HERG (0.0375–0.375 ng/nl), or 40 nl of cRNA in combination with both WT (0.0375 ng/nl) and S818L (0.0375, 0.1125 and 0.375 ng/nl) using a 10 μl Drummond micropipetter modified for microinjection (Drummond Scientific). Injected oocytes were incubated for 3–5 days at 14–16°C in modified Barth's solution containing (mmol/l) 88 NaCl, 1 KCl, 2.4 $NaHCO_3$, 15 Tris, 0.3 $Ca(NO_3)_2$, 0.4 $CaCl_2$, 0.8 $MgSO_4$, 100 μg/ml sodium penicillin, and 100 μg/ml streptomycin sulfate (pH 7.6 with HCl).

Membrane currents were recorded from oocytes by the conventional two-microelectrode voltage-clamp technique using an amplifier (GeneClamp 500, Axon Instruments) at a room temperature of 24–26°C. Current injecting and potential measuring electrodes had resistances of 0.5–1.5 MΩ when filled with 3 mol/l KCl. Current measurements were low-pass filtered at 0.5 kHz. Data acquisition and analysis were done using pClamp software (version 7, Axon Instruments) and a TL-1A/D converter (Axon Instruments). Oocytes were perfused continuously with a modified ND96 solution, containing (mmol/l) 96 NaCl, 2 KCl, 2.6 $MgCl_2$, 0.18 $CaCl_2$ and 5 HEPES (pH 7.6 with NaOH). A P/4 method was used to subtract leak and capacitative currents, unless otherwise indicated. All pulse protocols are indicated in the figure legends.

2.3. Data analyses

pCLAMP software (Axon Instruments) was used to measure current amplitude. To determine the voltage dependence of HERG current activation, a least-squares algorithm on Origin software (Microcal) or Excel software (Microsoft) was used to fit tail current amplitudes (I_{tail}) to a Boltzmann function in the following form:

$$I_{tail} = I_{tail-max} - I_{tail-max}/\{1 + \exp[(V_t - V_{1/2})/K]\}$$

where $I_{tail-max}$ is peak I_{tail}, V_t is the test potential, $V_{1/2}$ is the voltage at which I_{tail} is half of $I_{tail-max,}$ and K is the slope factor.

Curve fittings were done with a least-squares algorithm on pCLAMP software (Axon Instruments) or Origin software (Microcal).

To examine the activation time course, we used the envelope of tail tests [16,25], and peak current amplitudes were fitted to a single exponential function on Origin software (Microcal).

Steady-state inactivation was analyzed as described previously [15,16,24]. Briefly, the corrected steady-state inactivation curves were fitted with a Boltzmann function in the following form:

$$I/(I_{max} - I_{min}) = 1/\{1 + \exp[(V_p - V_{1/2})/K]\} + I_{min}$$

where I is the amplitude of inactivating current corrected for deactivation, I_{max} is the maximum of I, I_{min} is the minimum of I, V_p is the prepulse potential, $V_{1/2}$ is the voltage at which I is half of I_{max}, and K is the inverse slope factor.

All the values are expressed as mean ± S.E.M. One-way analysis of variance followed by a Student's t-test was used to test for significance ($P < 0.05$).

3. Results

3.1. S818L HERG alone could not form functional channels

First, we injected various amounts of S818L cRNA into *Xenopus* oocytes. Although we injected up to 15 ng S818L cRNA into oocytes, membrane currents were not different from those in H_2O-injected oocytes (Fig. 1). This indicated that S818L alone could not form functional channels.

3.2. S818L HERG did not exhibit apparent dominant-negative suppression

Next, as reported previously [14–16], we injected equal amounts (1.5 ng) of WT cRNA and S818L cRNA together into oocytes, which would render quantitative analysis feasible, and examined the characteristics of the expressed currents.

Fig. 2A,B displays representative traces of expressed currents in oocytes injected with 1.5 ng WT cRNA (WT1.5), and 1.5 ng WT cRNA plus 1.5 ng S818L cRNA (S818L/WT). Amplitudes of expressed currents for S818L/WT were similar to those for WT1.5 (Fig. 2C,D). The amplitude of expressed currents measured at −70 mV following depolarizing test pulses to +20 mV for S818L/WT (1620 ± 127 nA, $n = 9$) was not much different from that for WT1.5 (1597 ± 249 nA, $n = 8$) (Fig. 2D). Thus, S818L did not suppress WT HERG channel function in a dominant-negative manner. One simple explanation for this is that S818L subunits cannot participate in tetramer formation. However, as shown in Fig. 2E, the voltage to achieve half activation ($V_{1/2}$) for S818L/WT

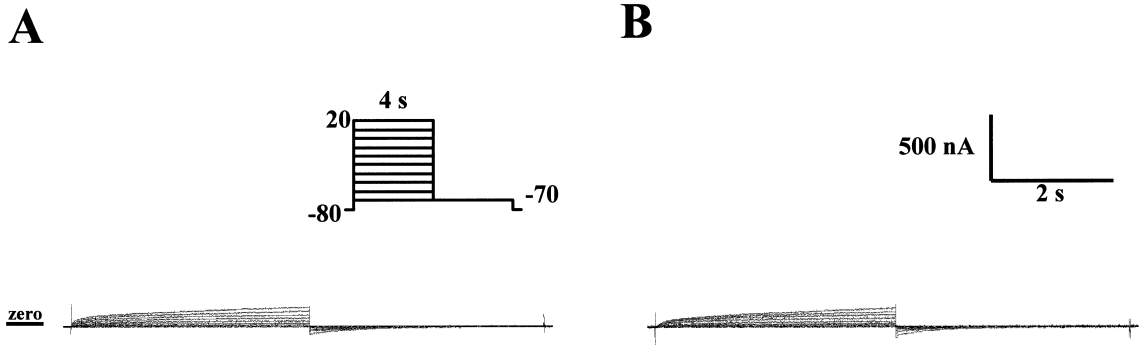

Fig. 1. No functional expression of the currents in oocytes injected with S818L HERG cRNA alone. Representative currents recorded in oocytes injected with 15 ng S818L cRNA (A) or with H_2O (B). Depolarizing test pulses were applied from a holding potential of −80 mV to various potentials between −70 and +20 mV in 10 mV increments for 4 s, followed by a hyperpolarizing pulse to −70 mV for 4 s. The voltage protocol is illustrated in the inset in A. Only endogenous currents were recorded. Small horizontal bar indicates zero current level.

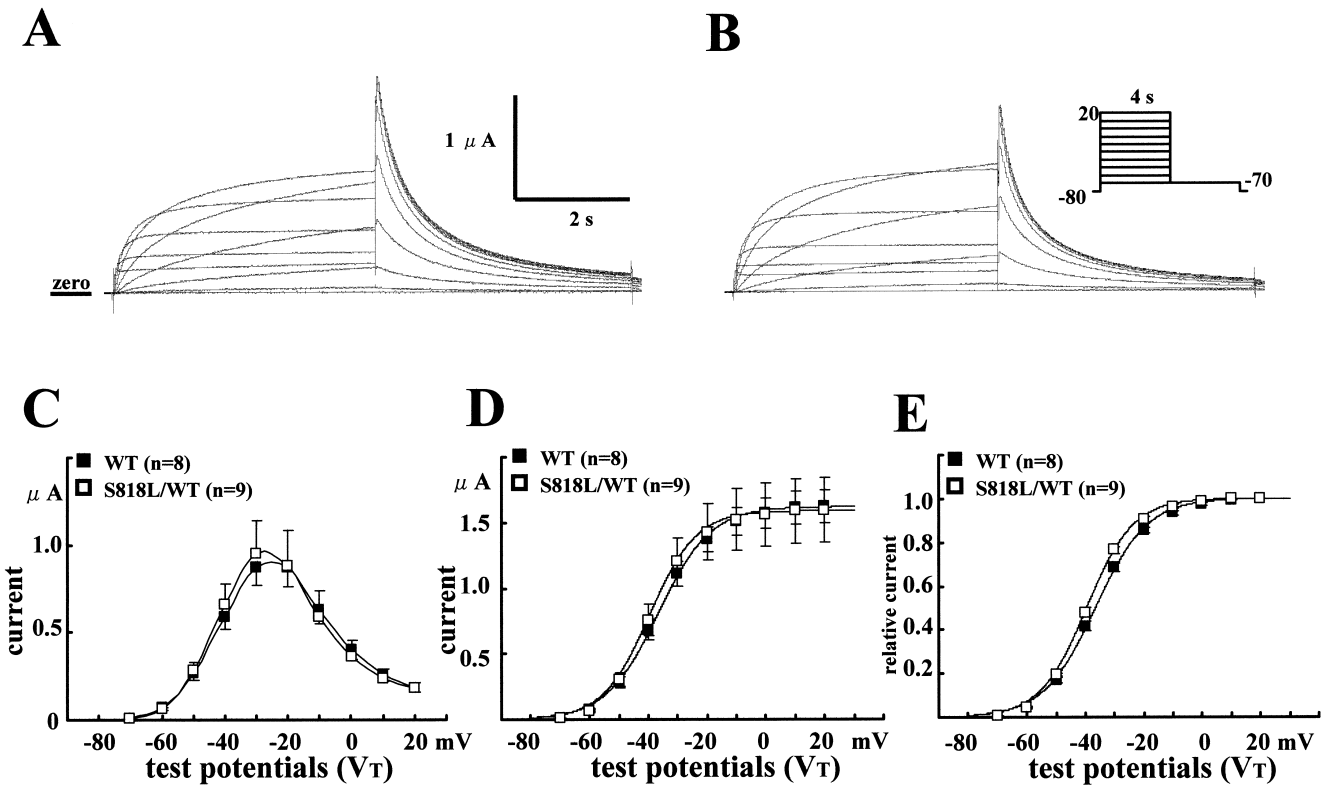

Fig. 2. No dominant-negative suppression by coinjection of equal amounts of S818L cRNA and WT cRNA. A,B: Expressed currents in oocytes injected with 1.5 ng WT cRNA (WT1.5) (A) or coinjected with 1.5 ng S818L cRNA and 1.5 ng WT cRNA (S818L/WT) (B). The voltage protocol is illustrated in the inset in B. C: Current–voltage (*I–V*) relationships for peak currents recorded during depolarizing pulses for WT1.5 (■) and S818L/WT (□). D: *I–V* relationships for amplitudes of tail currents for WT1.5 and S818L/WT. E: Normalized *I–V* relationships for amplitudes of tail currents for WT1.5 and S818L/WT.

(−39.6 ± 0.7 mV, $n = 9$) was shifted to negative potentials compared with that for WT1.5 (−36.6 ± 0.7 mV, $n = 8$) ($P < 0.05$). The slope factor (K) for S818L/WT (−7.8 ± 0.2 mV, $n = 9$) was reduced compared with that for WT1.5 (−8.9 ± 0.3 mV, $n = 8$) ($P < 0.05$). This finding appeared to suggest that, although S818L did not cause dominant-negative suppression, S818L might coassemble with the WT HERG channel and affect its voltage dependence of activation. To further inquire into this possibility, we examined the effects of excess amounts of S818L cRNAs on WT HERG channel properties.

3.3. Excess amounts of S818L cRNAs decreased HERG current amplitude and modified gating properties

We injected a 3-fold (4.5 ng) and a 10-fold (10 ng) excess of S818L cRNAs in combination with WT cRNA (1.5 ng) into oocytes (3-S818L/WT, 10-S818L/WT, respectively) and examined the expressed currents. Fig. 3A–C displays representative traces of expressed currents for WT1.5, 3-S818L/WT and 10-S818L/WT. Amplitudes of expressed currents for 3-S818L/WT and 10-S818L/WT were smaller than those for WT1.5 (Fig. 3D,E), whereas amplitudes of expressed currents in oocytes injected with a 10-fold WT cRNA (15 ng) were much larger than those for WT1.5 (data not shown). The amplitudes of expressed currents measured at −70 mV following depolarizing test pulses to +20 mV for 3-S818L/WT (845 ± 111 nA, $n = 8$) and 10-S818L/WT (597 ± 161 nA, $n = 8$) were significantly smaller than that for WT1.5 (1918 ± 225 nA, $n = 8$) (Fig. 3E). Moreover, the $V_{1/2}$ for 3-S818L/WT (−38.6 ± 0.6 mV, $n = 8$) and 10-S818L/WT (−40.7 ± 0.6 mV, $n = 8$) were shifted significantly to negative potentials compared with that for WT1.5 (−36.5 ± 0.8, $n = 8$), and the K for 3-S818L/WT (−7.5 ± 0.3 mV, $n = 8$) and 10-S818L/WT (−6.7 ± 0.3 mV, $n = 8$) were reduced significantly compared with that for WT1.5 (−8.8 ± 0.3 mV, $n = 8$) (Table 1, Fig. 3F). These changes in 10-S818L/WT were more prominent than those in 3-S818L/WT. Thus, since excess amounts of S818L cRNAs decreased HERG current amplitude and modified the voltage dependence of activation, we examined the effect of excess amounts of S818L cRNAs on other HERG channel kinetics.

We evaluated the activation time course of expressed currents using the envelope of tail protocol [16,25]. Fig. 4A,B displays representative traces of expressed currents for WT1.5 and 10-S818L/WT obtained by the envelope of tail protocol. Fig. 4C represents the normalized tail current amplitudes measured at an activation voltage of 0 mV for WT1.5, 3-S818L/WT and 10-S818L/WT. The activation time

Table 1
Parameters of activation for WT1.5, 3-S818L/WT, 10-S818L/WT

	Activation		
	Tail (nA)	$V_{1/2}$ (mV)	K (mV)
WT1.5	1918 ± 225	−36.5 ± 0.8	−8.8 ± 0.3
3-S818L/WT	845 ± 111*	−38.6 ± 0.6*	−7.5 ± 0.3*
10-S818L/WT	597 ± 161*	−40.7 ± 0.6*	−6.7 ± 0.3*

Tail: amplitude of tail current measured at −70 mV following depolarizing test pulse to +20 mV. $n = 8$. *$P < 0.05$, 3-S818L/WT, 10-S818L/WT versus WT1.5.

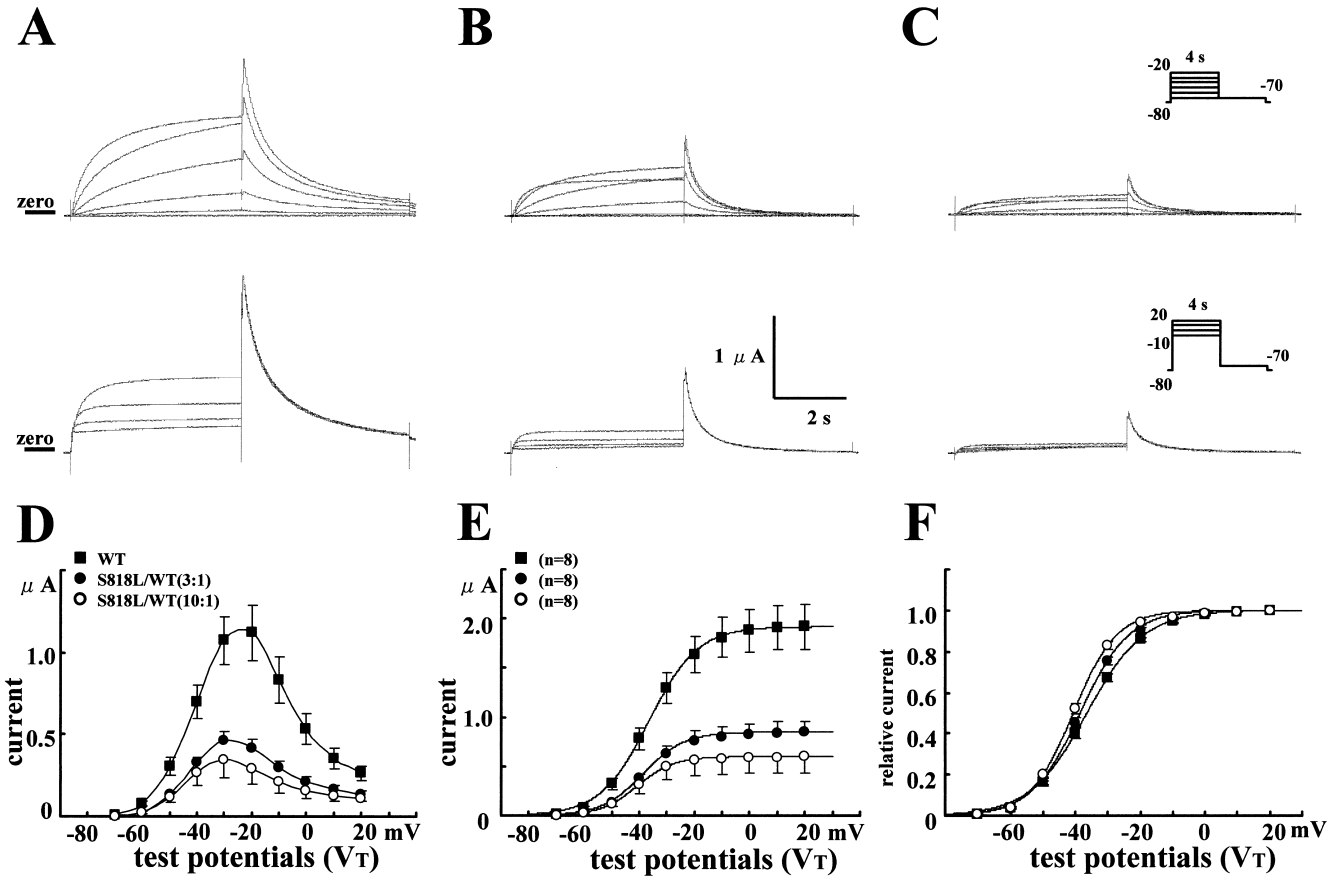

Fig. 3. Modification on the HERG current by coinjection of excess amounts of S818L cRNAs with WT cRNA. A–C: Expressed currents for WT1.5 (A), those coinjected with 3-fold (4.5 ng) S818L cRNA and 1.5 ng WT cRNA (3-S818L/WT) (B), those coinjected with 10-fold (15 ng) S818L cRNA and 1.5 ng WT cRNA (10-S818L/WT) (C). The voltage protocol is illustrated in the inset in C. Upper panels: depolarizing test pulses between −70 and −20 mV; lower panels: depolarizing test pulses between −10 and +20 mV. D: *I–V* relationships for peak currents recorded during depolarizing pulses for WT1.5 (■), 3-S818L/WT (●) and 10-S818L/WT (○). E: *I–V* relationships for amplitudes of tail currents for WT1.5, 3-S818L/WT and 10-S818L/WT. F: Normalized *I–V* relationships for amplitudes of tail currents for WT1.5, 3-S818L/WT and 10-S818L/WT.

course for 10-S818L/WT appeared to be accelerated compared with that for WT1.5. To compare the activation time course simply, we fitted tail currents to a single exponential function [16]. Although the activation time constants for S818L/WT and 3-S818L/WT were not much different from those for WT1.5, the activation time constants for 10-S818L/WT at each depolarizing potential were significantly smaller than those for WT1.5 (Fig. 4D). Thus, a 10-fold excess of S818L cRNA accelerated the activation time course of the HERG channel.

To analyze accurately the deactivation time course, long hyperpolarizing test pulses were applied after a depolarizing conditioning pulse (Fig. 5A). Fig. 5B represents superimposed traces of expressed currents for WT1.5 and 3-S818L/WT. Deactivating currents for 3-S818L/WT appeared to be accelerated compared with those for WT1.5. Deactivating currents during test pulses could be fitted to a double exponential function. At all test potentials, the fast and slow time constants for 3-S818L/WT and 10-S818L/WT were significantly smaller than those for WT1.5 (Fig. 5C,D). Thus, excess amounts of S818L cRNAs accelerated the deactivation time course of the HERG channel.

The steady-state inactivation was evaluated using a double pulse protocol as described previously [15,16,24]. Fig. 6 shows the steady-state inactivation curves for WT1.5, 3-S818L/WT and 10-S818L/WT. The voltage dependence of steady-state inactivation for 3-S818L/WT and 10-S818L/WT ($V_{1/2}$ values were -87.2 ± 1.7 mV [$n = 8$], and -85.7 ± 0.9 mV [$n = 8$], respectively) were not much different from that for WT1.5 ($V_{1/2}$: -86.2 ± 3.9 mV [$n = 6$]). Inverse slope factors for 3-S818L/WT and 10-S818L/WT (-30.6 ± 1.3 mV [$n = 8$], and -31.0 ± 1.2 mV [$n = 8$], respectively) were also comparable with that for WT1.5 (-30.1 ± 1.0 mV [$n = 6$]). Thus, excess amounts of S818L cRNAs did not affect the steady-state inactivation of HERG channel.

We next evaluated the time course of inactivation (test pulses: −40 to +20 mV) and recovery from inactivation (test pulses: −130 to −50 mV) as described previously [15,16]. At all test potentials, the time constants of inactivation and recovery from inactivation for 3-S818L/WT and 10-S818L/WT were not much different from those for WT1.5. Thus, the time course of inactivation and recovery from inactivation were not affected by excess amounts of S818L cRNAs (data not shown).

4. Discussion

4.1. Characterization of the loss of HERG channel function by S818L mutation

The role of the C-terminus on HERG channel function is

not yet clarified, mainly because none of the reported mutants in the *HERG* C-terminus can form functional homotetrameric channels, jeopardizing the kinetic analyses. The S818L mutation also cannot form functional homotetrameric channels. However, new insight into the effects of the *HERG* C-terminus on HERG channel kinetics could be provided by the coinjection experiments of S818L cRNA and WT HERG cRNA. While coinjection of equal amounts of S818L cRNA with WT cRNA into oocytes did not exhibit apparent dominant-negative suppression, coinjection of excess amounts of S818L cRNAs with WT cRNA into oocytes decreased HERG current amplitudes and shifted the voltage dependence of activation to negative potentials, accelerated its activation and deactivation, suggesting that S818L subunits can, at least in part, coassemble with WT subunits to form heterotetrameric functional channels.

These findings resemble the observations of a *HERG* C-terminal splice variant (HERGuso) reported by Kupershmidt et al. [26]. They reported that HERGuso, which is abundantly expressed in human heart, modified HERG current by decreasing its amplitude, accelerating its activation, and shifting the voltage dependence of activation to negative potentials when WT HERG cDNA and a 10-fold excess of HERGuso cDNA were cotransfected heterologously to a mammalian cell line. The similarity of the behaviors between mutant S818L and HERGuso may support the notion that the *HERG* C-terminus includes a domain critical for faithful recapitulation of the HERG/I_{Kr} current. In addition, the *HERG* C-terminus may contain a domain involving the activation–deactivation process of the channel. For other voltage-dependent potassium channels with six transmembrane domains, the importance of the C-terminus just downstream of the sixth transmembrane domain for channel activation–deactivation is also claimed [27]. These findings may provide the molecular clue for elucidating structure–function relationships of the *HERG* C-terminus.

What are the possible molecular mechanisms underlying the finding that not equal amounts of S818L cRNA but excess amounts of S818L cRNAs modified HERG currents? There could be some potential explanations; S818L cRNA is not equally translated or rapidly degrades compared with WT cRNA. Alternatively, S818L protein is not equally synthesized or rapidly degrades compared with WT protein. Zhou et al. [17] have reported that Y611H protein rapidly degrades compared with WT HERG protein. And recently, Kagan et al. [22] reported that coexpression of A561V with WT HERG reduces the WT HERG protein expression level by decreasing WT HERG protein synthesis and increasing its turnover rate. It remains to be determined, however, if S818L also acts in the same manner as Y611H or A561V. To delineate these possibilities, Western blotting and/or pulse chase analysis may be required.

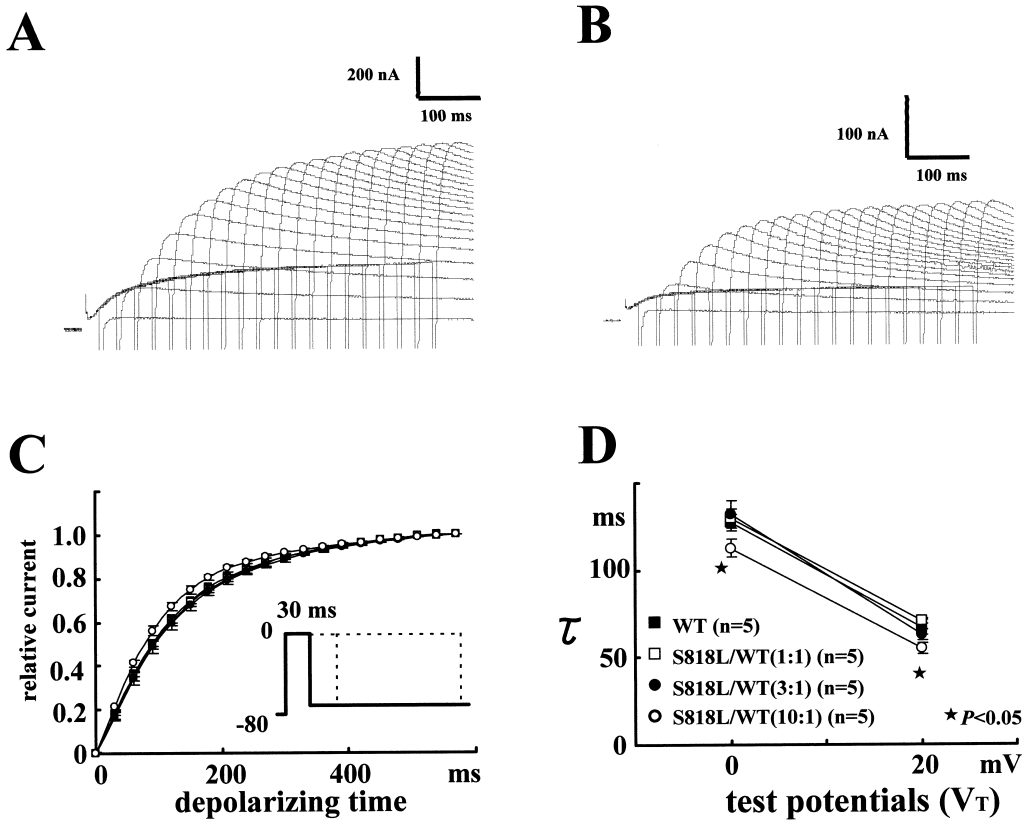

Fig. 4. Acceleration of the HERG current activation by coinjection of a 10-fold excess of S818L cRNA with WT cRNA. A,B: Superimposed traces of expressed currents for WT1.5 (A) and for 10-S818L/WT (B). A conditioning pulse to activation voltage (0, 20 mV) from a holding potential of −80 mV for varying durations of time from 30 to 600 ms in 30 ms increments was applied, followed by repolarization to −70 mV. The voltage protocol is illustrated in the inset in C. Currents were not leak-subtracted. Note that scale bars for current amplitudes differ between A and B. C: Normalized tail currents at an activation voltage of 0 mV for WT1.5 (■), S818L/WT (□), 3-S818L/WT (●), and 10-S818L/WT (○). D: Plots of activation time constants as a function of depolarized test potentials. Expressed tail currents for WT1.5, S818L/WT, 3-S818L/WT and 10-S818L/WT could be fitted with a single exponential function. ★$P < 0.05$, S818L/WT, 3-S818L/WT, 10-S818L/WT versus WT1.5.

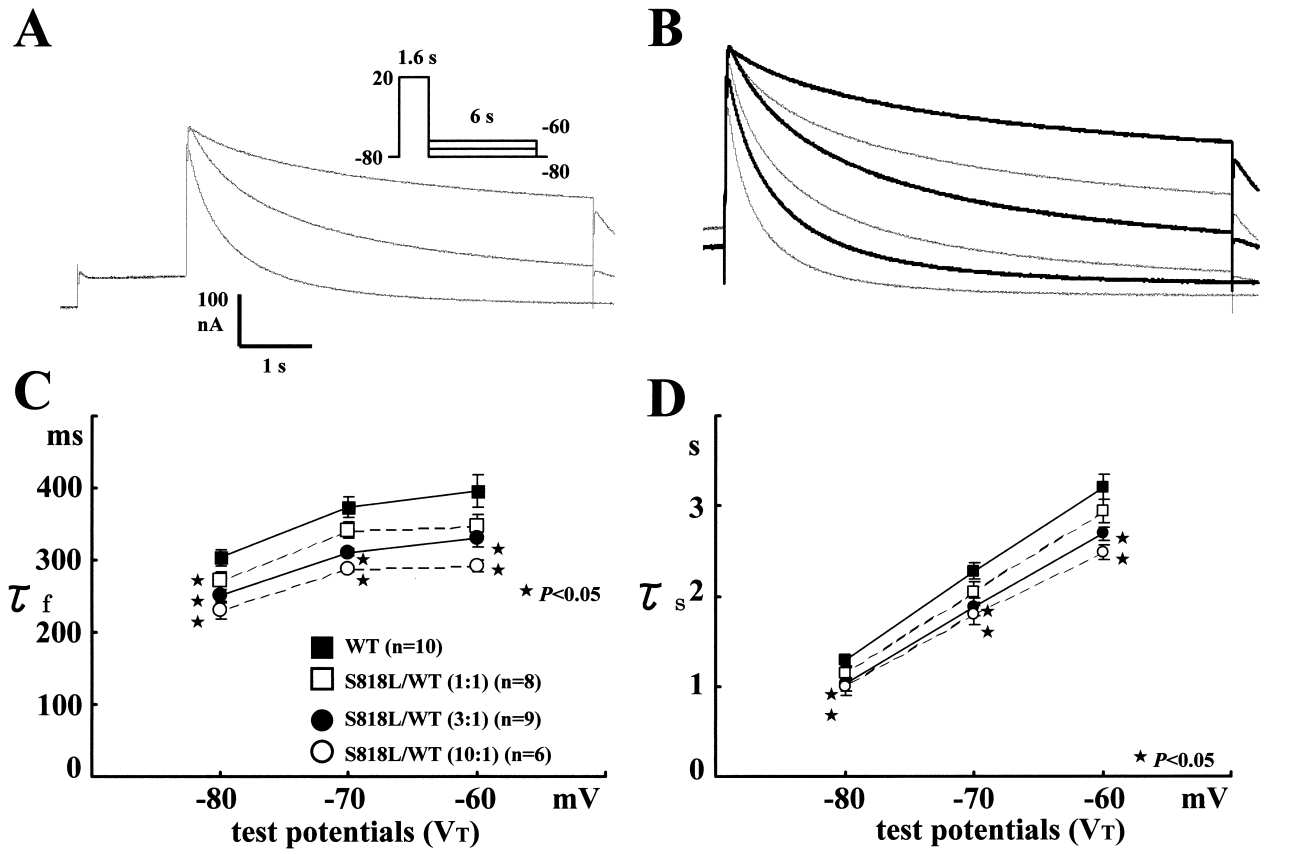

Fig. 5. Acceleration of the HERG current deactivation by coinjection of excess amounts of S818L cRNAs with WT cRNA. A,B: Representative currents were those for WT1.5 (A). Superimposed traces of expressed currents for WT1.5 and 3-S818L/WT (B). Expressed currents for WT1.5 are represented by bold lines and those for 3-S818L/WT are represented by thin lines. Note that the peak amplitude for 3-S818L/WT was fitted to that for WT1.5. A conditioning pulse to +20 mV for 1.6 s from a holding potential of −80 mV was applied, followed by hyperpolarizing test pulses between −80 and −60 mV in 10 mV increments for 6 s. The voltage protocol is illustrated in the inset in A. Currents were not leak-subtracted. Deactivation time constants were measured by fitting deactivating currents during test pulses at each potential with double exponentials. C,D: Fast (C) and slow (D) components of deactivation time constants for WT1.5 (■), S818L/WT (□), 3-S818L/WT (●) and 10-S818L/WT (○) as a function of test potentials. ★$P < 0.05$, S818L/WT, 3-S818L/WT, 10-S818L/WT versus WT1.5.

4.2. *Mechanism for prolongation of cardiac repolarization by the S818L mutation*

When equal amounts of S818L cRNA and WT cRNA, which would render quantitative analysis feasible, were coinjected into oocytes, the S818L mutation did not exhibit apparent dominant-negative suppression, and did not much affect the gating properties of the HERG channel. Thus, in this mutant, reduction of the quantitative HERG current may be the underlying mechanism for depressing the outward HERG current.

Our present and previous studies indicate that the degree of HERG current suppression in mutations in the *HERG* C-terminus is less severe than those in mutations in the pore region [15]. These data are compatible with the clinical data that mutations in the *HERG* C-terminus may be less malignant than mutations occurring in the pore region [23].

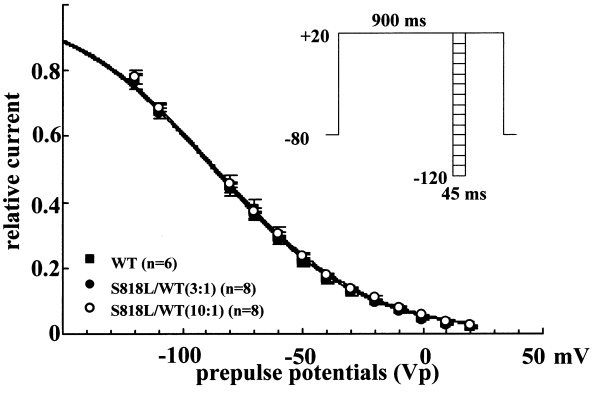

Fig. 6. Coinjection of excess amounts of S818L cRNAs with WT cRNA did not affect the steady-state inactivation of HERG channel. To examine steady-state inactivation, prepulse potentials between −120 mV and +20 mV in 10 mV increments for 45 ms were applied after a depolarizing pulse to +20 mV for 900 ms, followed by a common test pulse to +20 mV. The voltage protocol is illustrated in the inset. The peak current amplitudes during test pulses were plotted as a function of the previous prepulse potentials (V_p). At negative potentials, the currents decline due to the significant closing of channels through deactivation. Thus, this was corrected for by extrapolating the falling phase back to the start of the negative prepulse potentials, and applying the same relative correction to the initial outward current during the test pulse. Normalized steady-state inactivation for WT1.5 (■), 3-S818L/WT (●) and 10-S818L/WT (○) as a function of the prepulse potentials was fitted to a Boltzmann function.

Acknowledgements: We thank Gail A. Robertson (University of Wisconsin) for supplying HERG cDNA. We also thank T. Uchiyama and A. Yoguchi for technical advice. This work was supported by the Vehicle Racing Commemorative Foundation and a Research Grant for Cardiovascular Diseases (11C-1) from the Ministry of Health and Welfare.

References

[1] Wang, Q., Curran, M.E., Splawski, I., Burn, T.C., Millholland, J.M., VanRaay, T.J., Shen, J., Timothy, K.W., Vincent, G.M., de Jager, T., Schwartz, P.J., Towbin, J.A., Moss, A.J., Atkinson, D.L., Landes, G.M., Connors, T.D. and Keating, M.T. (1996) Nature Genet. 12, 17–23.
[2] Curran, M.E., Splawski, I., Timothy, K.W., Vincent, G.M., Green, E.D. and Keating, M.T. (1995) Cell 80, 795–803.
[3] Wang, Q., Shen, J., Splawski, I., Atkinson, D., Li, Z., Robinson, L.J., Moss, A.J., Towbin, J.A. and Keating, M.T. (1995) Cell 80, 805–811.
[4] Schott, J.J., Charpentier, F., Peltier, S., Foley, P., Drouin, E., Bouhour, J.B., Donnelly, P., Vergnaud, G., Bachner, L., Moisan, J.P., Le Marec, H. and Pascal, O. (1995) Am. J. Hum. Genet. 57, 1114–1122.
[5] Splawski, I., Firouzi, M.T., Lehmann, M.H., Sanguinetti, M.C. and Keating, M.T. (1997) Nature Genet. 17, 338–340.
[6] Warmke, J.W. and Ganetzky, B. (1994) Proc. Natl. Acad. Sci. USA 91, 3438–3442.
[7] Sanguinetti, M.C. and Jurkiewicz, N.K. (1990) J. Gen. Physiol. 96, 195–215.
[8] Sanguinetti, M.C., Jiang, C., Curran, M.E. and Keating, M.T. (1995) Cell 81, 299–307.
[9] Benson, D.W., MacRae, C.A., Vesely, M.R., Walsh, E.P., Seidman, J.G., Seidman, C.E. and Satler, C.A. (1996) Circulation 93, 1791–1795.
[10] Satler, C.A., Walsh, E.P., Vesely, M.R., Plummer, M.H., Ginsburg, G.S. and Jacob, H.J. (1996) Am. J. Med. Genet. 65, 27–35.
[11] Dausse, E., Berthet, M., Denjoy, I., Andre-Fouet, X., Cruaud, C., Bennaceur, M., Faure, S., Coumel, P., Schwartz, K. and Guicheney, P. (1996) J. Mol. Cell. Cardiol. 28, 1609–1613.
[12] Tanaka, T., Nagai, R., Tomoike, H., Takata, S., Yano, K., Yabuta, K., Haneda, N., Nakano, O., Shibata, A., Sawayama, T., Kasai, H., Yazaki, Y. and Nakamura, Y. (1998) Circulation 95, 565–567.
[13] Itoh, T., Tanaka, T., Nagai, R., Kamiya, T., Sawayama, T., Nakayama, T., Tomoike, H., Sakurada, H., Yazaki, Y. and Nakamura, Y. (1998) Hum. Genet. 102, 435–439.
[14] Sanguinetti, M.C., Curran, M.E., Spector, P.S. and Keating, M.T. (1996) Proc. Natl. Acad. Sci. USA 93, 2208–2212.
[15] Nakajima, T., Furukawa, T., Tanaka, T., Katayama, Y., Nagai, R., Nakamura, Y. and Hiraoka, M. (1998) Circ. Res. 83, 415–422.
[16] Nakajima, T., Furukawa, T., Hirano, Y., Tanaka, T., Sakurada, H., Takahashi, T., Nagai, R., Itoh, T., Katayama, Y., Nakamura, Y. and Hiraoka, M. (1999) Cardiovasc. Res. 44, 283–293.
[17] Zhou, Z., Gong, Q., Epstein, M.L. and January, C.T. (1998) J. Biol. Chem. 273, 21061–21066.
[18] Furutani, M., Trudeau, M.C., Hagiwara, N., Seki, A., Gong, Q., Zhou, Z., Imamura, S., Nagashima, H., Kasanuki, H., Takao, A., Momma, K., January, C.T., Robertson, G.A. and Matsuoka, R. (1999) Circulation 99, 2290–2294.
[19] Chen, J., Zou, A., Splawski, I., Keating, M.T. and Sanguinetti, M.C. (1999) J. Biol. Chem. 274, 10113–10118.
[20] Lees-Miller, J.P., Duan, Y., Teng, G.Q., Thorstad, K. and Duff, H.J. (2000) Circ. Res. 86, 507–513.
[21] Li, X., Xu, J. and Li, M. (1997) J. Biol. Chem. 272, 705–708.
[22] Kagan, A., Yu, Z., Fishman, G.I. and McDonald, T.V. (2000) J. Biol. Chem. 275, 11241–11248.
[23] Berthet, M., Denjoy, I., Donger, C., Demay, L., Hammoude, H., Klug, D., Schulze-Bahr, E., Richard, P., Funke, H., Schwartz, K., Coumel, P., Hainque, B. and Guicheney, P. (1999) Circulation 99, 1464–1470.
[24] Smith, P.L., Baukrowitz, T. and Yellen, G. (1996) Nature 379, 833–836.
[25] Wang, S., Liu, S., Morales, M.J., Strauss, H.C. and Rasmusson, R.L. (1997) J. Physiol. 502, 45–60.
[26] Kupershmidt, S., Snyders, D.J., Raes, A. and Roden, D.M. (1998) J. Biol. Chem. 273, 27231–27235.
[27] Liu, Y., Holmgren, M., Jurman, M.E. and Yellen, G. (1997) Neuron 19, 175–184.